WELDING RESEARCH

SUPPLEMENT TO THE *WELDING JOURNAL*, FEBRUARY 1995
Sponsored by the American Welding Society and the Welding Research Council

The Role of Failure Mode, Resistance Spot Weld and Adhesive on the Fatigue Behavior of Weld-Bonded Aluminum

Aluminum joined with a combination of welding and adhesive bonding displays a higher fatigue strength than either aluminum or steel spot welds

BY P. C. WANG, S. K. CHISHOLM, G. BANAS, AND F. V. LAWRENCE, Jr.

ABSTRACT. Fatigue behavior of the weld-bonded (combination of welding and adhesive bonding) aluminum joint was investigated as part of a study attempting to replace steel with aluminum in the lightweight vehicle structure. Aluminum 5754-H40 alloy and bis-phenol-A epoxy adhesive were used in specimen fabrication. Test results showed that weld-bonded aluminum had a slightly lower fatigue resistance than the adhesive-bonded aluminum (*i.e.*, the presence of the resistance spot weld decreases the fatigue strength by 11% at 3 x 10^6 cycles) but a much higher fatigue resistance than the aluminum and steel spot welds. Microscopic examinations showed that failure of weld-bonded aluminum occurred by either "nugget-through" where failure originated from the weld nugget, or "adherend-tearing" where failure started from the edge of adherend overlap. Statistical analyses of the test results of weld-bonded aluminum indicated that fatigue strength is not significantly affected by the failure modes.

P. C. WANG is with the Physics Department, Research and Development Center, General Motors Corp., Warren, Mich. S. K. CHISHOLM is with the Ford Motor Co., Dearborn, Mich. G. BANAS and F. V. LAWRENCE, Jr., are with the University of Illinois at Urbana-Champaign, Urbana, Ill.

Introduction

Recent advances in weld bonding (a combination of resistance welding and adhesive bonding) technology have accelerated the use of aluminum alloys for lightweight vehicle structures. Aluminum has the advantages of low density and good corrosion resistance when compared with steel. Also, there is a secondary benefit: lighter vehicle bodies mean that other parts such as springs, shocks, frame, tanks, and engine can be lighter and smaller. As a result, weld bonding aluminum can become a very attractive technology in vehicle fabrication.

KEY WORDS

Aluminum Alloys
Weld-Bonded Al
Fatigue Strength
Lightweight Vehicles
Resistance Welding
Adhesive Bonding
Failure Modes
Microhardness
Fractography
Statistical Analysis

However, even with all the potential advantages of weld bonding, vehicle manufacturers still hesitate to use this technology in primary structural components. This reluctance is due, in part, to the lack of understanding of the failure mode and durability of weld-bonded joints. Several studies have been reported on the static (Refs. 1, 2) and fatigue (Refs. 3, 4) strengths of weld-bonded aluminum joints; however, very little information is available on their failure modes.

In this study, we address the fatigue strengths and failure modes of weld-bonded lap joints. For comparison purposes, the adhesive-bonded and resistance spot-welded joints are also included in this study. Figure 1A–C shows the weld-bonded, adhesive-bonded and resistance spot-welded specimens, respectively. The specimens were tested under constant amplitude cyclic loading in an ambient laboratory environment. Fatigue test results of weld-bonded joints are presented, and compared with those of the steel spot weld. Failure modes and fracture surfaces of fatigued specimens were examined using optical and scanning electron microscopes (SEM). Statistical analysis was used to check the effect

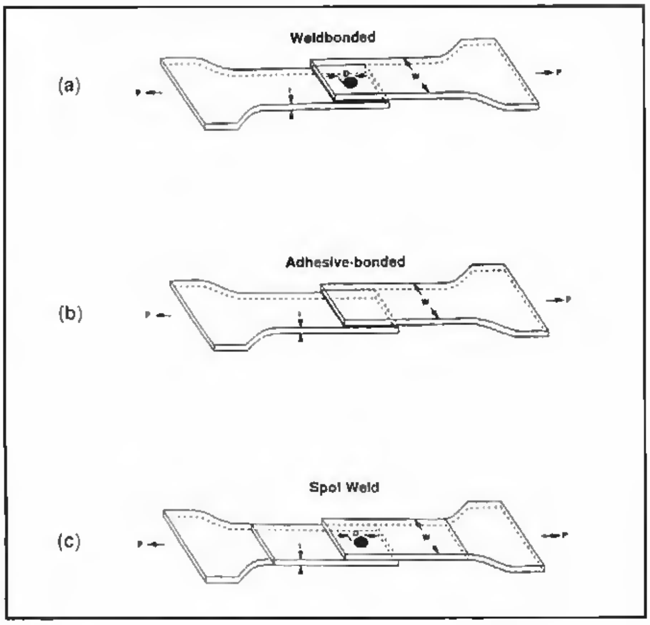

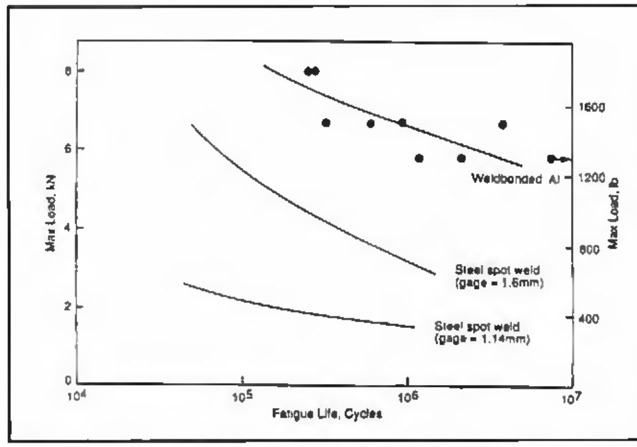

Fig. 2 — Fatigue test results for weld-bonded aluminum joints. Steel spot weld data are from Ref. 7.

Fig. 1 — Schematic of a lap-shear. A — Weld-bonded joint; B — adhesive-bonded joint; C — resistance spot welded joint.

of failure mode on fatigue resistance of weld-bonded joints. Finally, we discuss the roles of the resistance spot weld and adhesive on fatigue behavior of weld-bonded joints.

Experimental Procedure

Material

Aluminum Alloy 5754-H40 (soft temper) 1.6 mm (0.063 in.) thick and an epoxy adhesive were used in this study. The aluminum alloy was surface treated using a proprietary process. A mixture of silicon-chromium oxide was coated on the aluminum surface to prevent the aluminum oxide from forming during welding and to enhance the adhesion between the adhesive and adherend. Nuclear magnetic resonance (NMR), Fourier transform infrared spectroscopy (FTIR), x-ray diffraction (XRD), polarized light microscopy, scanning electron (SEM) and transmission electron microscopy (TEM) analyses of the epoxy adhesive showed that it is composed of bis-phenol-A epoxy resin, fumed silica, quartz and wollastonite (*i.e.*, $CaSiO_3$) (Ref. 5). The curing agent appears to be an amine compound. Tensile properties of aluminum alloy and epoxy adhesive are given in Tables 1 and 2, respectively.

Specimen Fabrication

The lap-shear specimens were fabricated from 38.1 x 127-mm (1.5 x 5-in.) coupons. Specimens were prepared by: 1) applying the one-part, heat curing, toughened adhesive, through a hand-held injection gun, on one of the two contact surfaces; 2) bringing adherends together; 3) positioning them with a fixture; 4) resistance spot welding the specimens (a resistance spot weld with a nugget diameter of 5 mm (0.2 in.) was centered on a 38.1-mm (1.5-in.) square overlap region. The weld nugget was then prepared using a single-phase, microprocessor-controlled AC electrical resistance welding unit. The welding schedule employed is given in Table 3; and 5) curing the specimens through a two-stage process (10 minutes at 145°C for wetting the adherend, and then 30 min at 175°C for cross-linking). All finished specimens were examined for the presence of any defects. In order to reduce the scatter in the data, the specimens with defects (*i.e.*, uneven bond-line thickness and pores at the adhesive fillet) were discarded. Similar procedures, with the exception of resistance spot welding, were used to prepare the adhesive-bonded specimens.

Microhardness Measurements

Weld-bonded specimens were sectioned perpendicular to the sheet thickness and polished so that hardness could be measured using a Knoop (Ref. 6) hardness tester. Hardness measurements were performed to reveal possible changes in material properties due to the heat from welding.

Fatigue Testing

Specimens were gripped in self-aligning hydraulic grips and then tested in an MTS testing machine under ambient laboratory conditions from zero to a tensile load ($R = 0$, where $R = min/max$ load). To minimize bending stresses during testing, both ends of the specimens were attached by adhesive to two filler plates of the same thickness. All fatigue tests were performed at 20 Hz frequency. Weld nugget "pull-out" (for resistance spot weld) or complete separation of the test piece (for adhesive-bonded and weld-bonded joints) into two pieces was de-

Table 1 — Tensile Properties[(a)] of Aluminum Alloy 5754-H40

	Longitudinal	Transverse
0.2% Yield strength, MPa (ksi)	126 (18.3)	115 (16.7)
Tensile strength, MPa (ksi)	227 (32.9)	220 (31.9)
% Elongation, in 50.8 mm (2 in.)	20.2	22.5
Strain hardening exponent, n	0.256	0.273

(a) Under a strain rate of 3.3×10^{-3}/s.

Table 2 — Tensile Properties[(a)] of the Bis-Phenol-A Epoxy Adhesive

Tensile modulus, GPa (ksi)	2.80 (406.4)
Tensile strength, MPa (ksi)	57.82 (8.39)
% Elongation at break	5.44

(a) Under a stroke rate of 0.01 mm/s.

Table 3 — Welding Parameters

Welding current (kA)	Welding time (cycle)	Electrode force (lb)	Electrode force (N)	Electrode cap
22.7	8	600	2,669	MWZ 6008

1 cycle = 1/60 s.

fined as failure. If a specimen did not fail, the test was terminated at about 5 to 10 million cycles.

Fractography

Post-failure fractographic analysis was performed with scanning electron microscopy to study the failure mechanisms. Specimens were cut from the broken overlap sections. Before SEM examination, each specimen was sputter coated with gold-palladium.

Results and Discussion

Fatigue Test Results

Fatigue test results for weld-bonded aluminum are plotted in Fig. 2 and listed in Table 4. For comparison purposes, fatigue data for 1.14-mm (0.045-in.) and 1.6-mm (0.063-in.) steel spot welds from the work of Abe, *et al.* (Ref. 7), are also plotted in Fig. 2. The steel spot welds with 1.14 mm gauge were selected because Glaser, *et al.* (Ref. 3), found that similar static strengths can be achieved for resistance spot-welded steel and weld-bonded aluminum alloy, where the aluminum sheet thickness is 1.4 times that of the steel. A best-fit curve was approximated through the data for each joint type. As shown, the weld-bonded specimens gave the highest fatigue resistance. Fatigue strengths at 3 x 10^6 cycles were approximately 4.5 and 1.57 times greater than the steel spot welds (with gauges 1.14 and 1.6 mm), respectively. The superior fatigue resistance of the weld-bonded specimens is due to the low local stress intensity as a result of the large bonded area.

Weld-bonded joints were shown to substantially out-perform the steel spot welds. It should be noted that data reported in this study were obtained under ambient laboratory conditions. Weld-bonded joints are susceptible to bond degradation by heat, moisture, and chemical attack (Ref. 8). Preliminary test results of weld-bonded specimens under the condition of 100% relative humidity (R.H.) at 38°C (100°F) showed that a 33% decrease in fatigue strength at 5 x 10^6 cycles was observed (Ref. 8). Because a low-amplitude cyclic load allows time for interaction between material and environment, the differences are expected to become more pronounced at the high cycle regimes.

Table 4 — Fatigue Test Results for Weld-Bonded Aluminum Joint

Specimen	Load (lb)	Load (N)	Fatigue Life (cycle)	Failure Mode
1	1,500	6,672	322,000	adherend-tearing
2	1,500	6,672	598,500	nugget-through
3	1,500	6,672	3,760,900	nugget-through
4	1,500	6,672	934,500	nugget-through
5	1,300	5,783	1,191,200	adherend-tearing
6	1,300	5,783	2,130,300	adherend-tearing
7	1,300	5,783	7,446,600	run-out
8	1,800	8,007	249,400	adherend-tearing
9	1,800	8,007	279,000	nugget-through
11	1,800	8,007	251,200	nugget-through

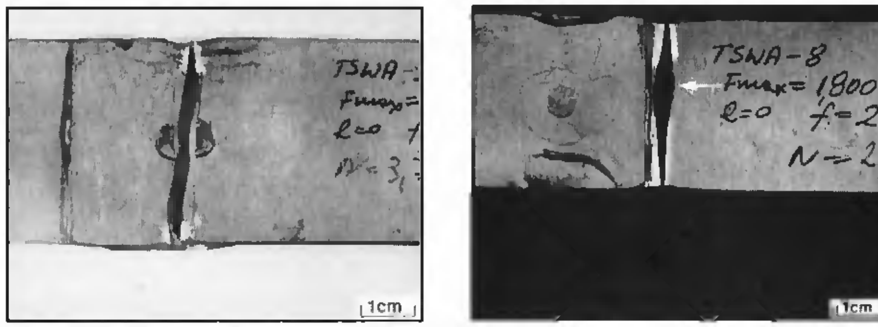

Fig. 3 — Fatigue failure mode for the weld-bonded aluminum joint. A — Nugget through; B — adherend tearing.

Fractographic Examination

Two fatigue failure modes were observed for weld-bonded specimens. Figure 3A shows the nugget-through failure mode where the cracks initiated from the welding discontinuities in the weld nugget and grew across the weld nugget with increasing number of cycles. Ultimate failure was by tensile overload of the remaining unseparated sections. Figure 4A shows a composite of three SEM views that were taken at the location of fatigue origin due to nugget-through fracture. As shown, the internal cavities in

Fig. 4 — Examination by SEM. A — Three views of a nugget-through weld-bonded specimen; B — higher magnification of area indicated by arrow in A.

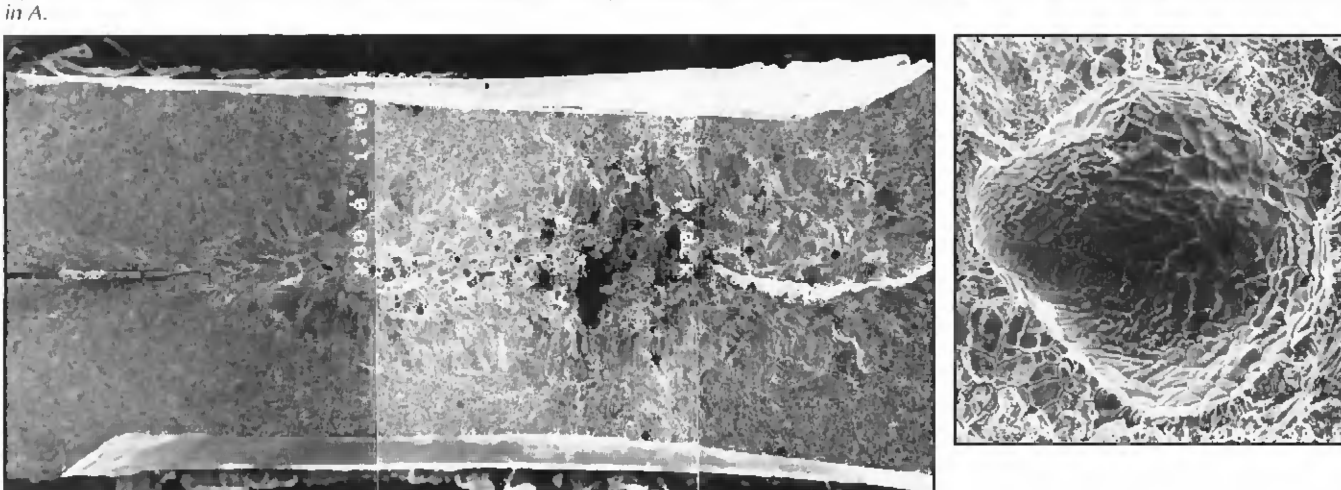

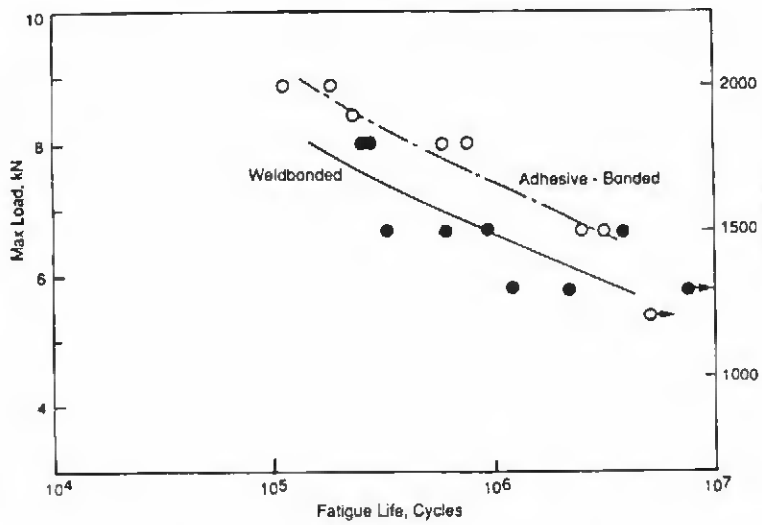

Fig. 5 — Comparison of fatigue resistance of adhesive-bonded and weld-bonded aluminum joints.

Fig. 6 — Matching-half fractographs of tensile tested aluminum joints. Top — Weld-bonded; Lower — adhesive-bonded.

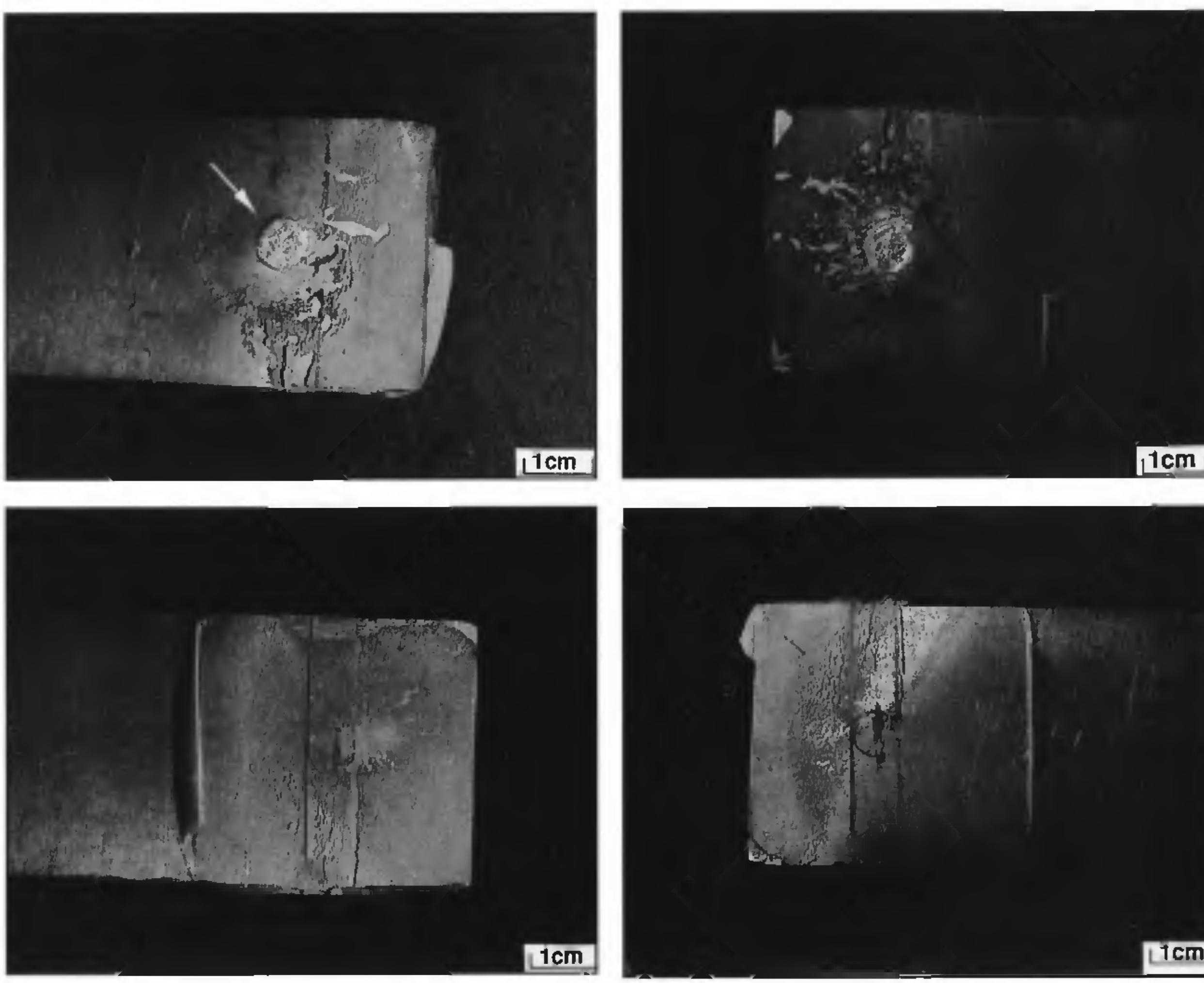

the weld nugget are apparent in the fractograph. Fatigue fracture occurs by growth of these cavities. The shapes of the cavities located in the middle of the weld nugget are very conducive to crack propagation with little plastic deformation. These cavities may result from too rapid heating of the weld metal and an excessively high cooling rate, or the shrinkage of metal during solidification. The rapid heating and high cooling rate may result in the hydrogen trapped in the weld nugget (Ref. 10). Hydrogen has high solubility in molten aluminum but very low solubility in solid aluminum. Hydrogen dissolved in the molten weld pool during welding is released during solidification. The high cooling rate can prevent the evolved hydrogen from rising to the surface of the weld pool, with the result that cavities occur. The likely sources of hydrogen are lubricant on the aluminum surface and moisture in the air. The shrinkage of aluminum during cooling from the liquidus temperature to room temperature also creates internal cavities. A view at higher magnification of the area indicated by an arrow in Fig. 4A is shown in Fig. 4B. This shows more clearly the dendritic structure of the cav-

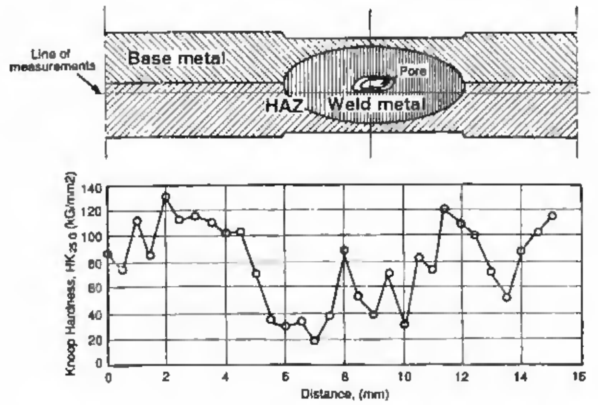

Fig. 7 — Microhardness vs. distance across the base metal, heat-affected zone and weld metal.

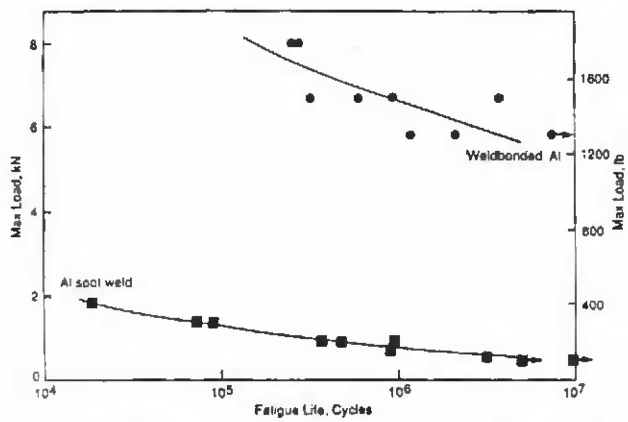

Fig. 8 — Comparison of fatigue resistance of weld-bonded and resistance spot-welded aluminum joints.

ity. The region in the cavity contains dendrite lobes, which existed as "free surface" within the cavities after the available liquid metal solidified. This behavior might have been caused by a lack of molten metal within the cavity.

Adherend-tearing mode is shown in Fig. 3B where the cracks originated from the edge of the overlap region and then grew across the adherend width. Visual examinations of adherend-tearing specimens showed that there was a debonding between adhesive and adherend. After debonding, fatigue crack initiated at the interface of adhesive and adherend, and then grew into the aluminum adherend. Crack observations during testing showed that a large portion of the fatigue life was devoted to debonding and crack growth at the interface. These results suggest that fatigue of weld-bonded joints with adherend-tearing failure mode is dominated by crack growth.

Effect of Failure Mode on Fatigue Strength

In order to check the effect of failure mode on fatigue resistance of weld-bonded joints, statistical analysis was used. Details of the test statistics are described in Ref. 11. For the sake of clarity and continuity, however, the relevant features of the test statistics are briefly recapitulated.

Let s_1 be the standard deviation in fatigue life for numbers of specimen (k_1) with nugget-through failure, and s_2 be the standard deviation in fatigue life for numbers of specimens (k_2) with adherend-tearing mode. The total standard deviation in fatigue life for all the specimens ($K = k_1 + k_2$) is defined as S. The test statistics for the analysis of variance is denoted F*:

$$F^* = \frac{(k_1-2)(S^2-s_1^2)+(k_2-2)(S^2-s_2^2)}{(K-2)(K-4)} \times \frac{(K-4)}{(k_1-2)s_1^2+(k_2-2)s_2^2} \quad (1)$$

The F* value obtained from Equation 1 is compared with tables of the F-distribution (Ref. 12). If the value of F* is greater than the F-value obtained from the statistical tables, the two sets of variances are significantly different at the chosen level of confidence. Fatigue test results and failure modes for each weld-bonded specimen are given in Table 4. An F* value of 1.77 was obtained using Equation 1. This is to be compared with 5.79, the F value for the sample size of 9 in Table 4 for 85% confidence level. This comparison shows that fatigue resistance of the weld-bonded joint is not significantly affected by the failure mode. A possible explanation of this result is that there is little difference in notch severity of specimens with nugget-through (from weld discontinuities) and adherend-tearing (from overlap edge) failure modes.

Role of Resistance Spot Weld on Fatigue Strength of Weld-Bonded Joint

While the resistance spot weld serves as a peel stopper for weld-bonded specimens under a peel load and a fastener to hold parts together during the curing stage, its role on tensile-fatigue strength of weld-bonded joints is not clear. The role of resistance spot welding on fatigue strength was determined by comparing the fatigue strengths of weld-bonded and adhesive bonded joints. Figure 5 gives the fatigue test results of weld-bonded and adhesive-bonded joints. Unlike the weld-bonded joints which failed by either nugget-through or adherend-tearing, adhesive-bonded joints failed only by adherend-tearing. As shown in Fig. 5, the fatigue strength is reduced by the presence of the resistance spot weld. At 3 x 10^6 cycles, weld-bonded joints show a 11% decrease in the fatigue strength when compared to adhesive-bonded joints. By combining Figs. 2 and 5, we see that weld-bonded joints had a slightly lower fatigue resistance than the simple adhesive-bonded joints but a much higher fatigue resistance than steel spot welds.

The reason why the fatigue strength of the weld-bonded joint is inferior to an adhesive-bonded joint is clearly seen in the fractographic results presented in Fig. 6. Figure 6A shows a set of matching-half fractographs of a tensile-tested, weld-bonded specimen. Note, that an unbonded area indicated by an arrow is visible around the weld nugget. The evolution of gases generated by the decomposition of the adhesive and silicon-chromium oxide coating during welding forced the adhesive from around the nugget and reduced the bonded area of the joint. As much as 7% to 8% of the surface available for bonding was actually unbonded in a typical weld-bonded specimen; whereas, the fractographs of a tensile-tested adhesive-bonded specimen shown in Fig. 6B indicated hardly any unbonded area. Finite element stress analyses of weld-bonded specimens showed that the presence of the unbonded area results in an increase in stresses at the periphery of the weld nugget and at the edge of the adherend overlap (Ref. 13). The high stresses could lead to fatigue crack growth from the weld cavities. Thus, the reduction of bonded area together with the presence

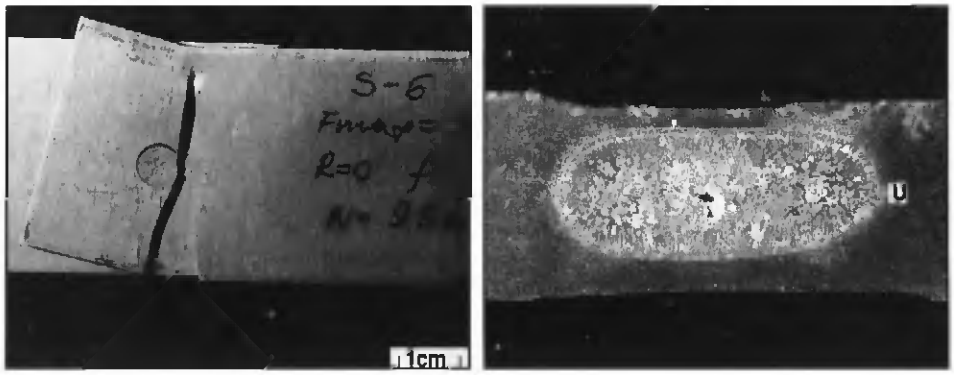

Fig. 9 — Resistance spot welds. Left — Weld nugget pull-out failure; Right — cross-section of untested aluminum joint.

of weld discontinuities (Fig. 4) are the main reasons for the fact that the weld-bonded specimens generally did not perform as well as the adhesive-bonded specimens.

Microhardness measurements provide a mechanical property of one kind (Ref. 14). Figure 7 shows the hardness measurements of base metal, heat affected-zone (HAZ) and weld metal. Weld metal and HAZ were found to have low hardness as compared with base metal. These differences are attributed to the heat from welding removing part of the effects of material strain hardening. In consequence, the fatigue strength of the HAZ and weld metal may not exceed that of the base metal. Since the fatigue cracks could initiate from the HAZ and weld metal, the low strengths of the HAZ and weld metal helped to further explain the weak fatigue resistance of weld-bonded specimens.

Role of Adhesive on Fatigue Behavior of Weld-Bonded Joints

In order to assess the role of adhesive on the fatigue behavior of weld-bonded joints, resistance spot-welded specimens were fabricated and tested. Figure 8 shows the fatigue test results for resistance spot-welded and weld-bonded joints. As shown, fatigue strength at 3 x 10^6 cycles was approximately 10 times greater than the resistance spot-welded aluminum. The superior fatigue resistance of the weld-bonded specimens is due to the low-stress concentration as a result of the large bonded area.

The adhesive not only improves the fatigue strength, but changes the failure mode completely. Figure 9A shows a typical weld nugget "pull-out" failure mode for a resistance spot-welded joint. Intermittent visual and optical examinations showed that fatigue cracks, instead of growing from cavities, grow from site U — Fig. 9B. They then propagated through the sheet thickness and also along the periphery of the weld nugget. Ultimate failure was by tensile overload of the remaining unseparated sections. A similar result was also found in steel spot welds (Ref. 15).

Figure 10A illustrates an appearance of fracture surface obtained with a maximum load of 534 N (120 lb). Fracture occurred at 3,194,900 cycles. A higher magnification of the dark region indicated by the arrow in Fig. 10A is shown in Fig. 10B. The fracture surface was covered with a dark coating (*i.e.*, silicon-chromium oxide). This dark coating may result from surface abrasion during cyclic loading of the fatigue test, and is likely a mixture of inorganic coating and debris of the aluminum alloy (Ref. 16). Fig. 10C is a higher magnification of the outlined region in Fig. 10A, which shows fatigue crack growth occurring by striation. As indicated, the fracture surface is characterized by fatigue striation (shown by arrows) and tearing. As shown, patches of fatigue striations are separated by narrow tear ridges, as at A. The pronounced variations in striation orientation indicate local changes in the direction of fatigue crack propagation. These results suggest stress-intensity levels that approach the fracture toughness, K_{Ic}, of the aluminum alloy. That is, crack depths approach that which corresponds to catastrophic fracture. Also shown in Fig. 10C, there are secondary cracks between the grain boundaries and precipitates.

The implications of the above test results and fractography are quite significant. First, as far as tensile-fatigue is concerned, weld-bonded aluminum may replace the steel spot welds. Secondly, the primary causes of the fatigue failure were identified, and based on this information, corrective action can be taken to improve the fatigue performance. For example, better control of welding schedules to reduce the internal cavities in the weld nugget and of adhesive fillets along the edge of the adherend overlap to minimize the local stress concentration could result in improved fatigue strength.

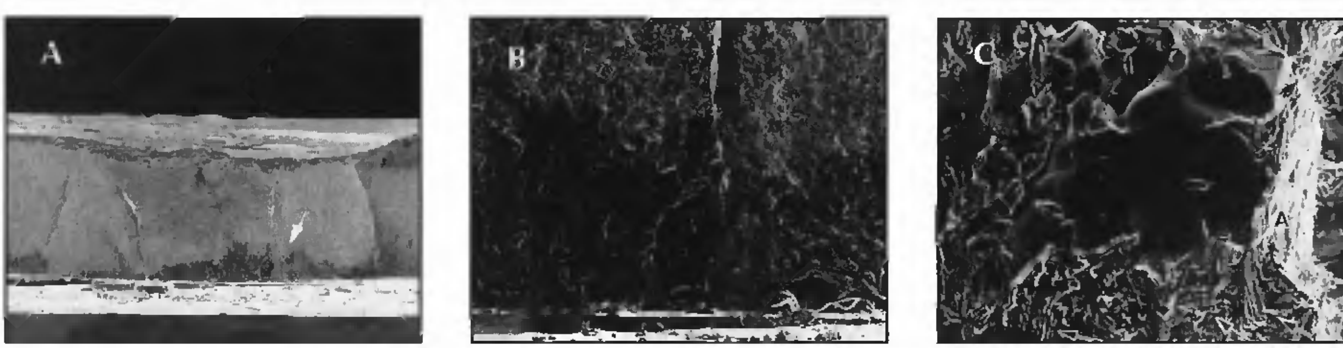

Fig. 10 — Scanning electron micrograph of a fatigued resistance spot-welded joint. A — At the region where the fatigue cracks intitiated; B — enlarged view of the region indicated by arrow; C — mixed fatigue striation (shown by arrows) and tearing. Not that the patches of fatigue striations are separated by narrow tear ridges, as at A.

Conclusions

The results of tensile-fatigue testing conducted on the aluminum 5754-H40 weld-bonded, adhesive-bonded and resistance spot-welded lap joints with a 38.1 mm^2 overlap region have provided the following conclusions:

1) Fatigue strengths of weld-bonded aluminum, at 3×10^6 cycles, were approximately 10, 4.5 and 1.57 times greater than the aluminum spot weld and steel spot welds (with gauges 1.14 and 1.6 mm), respectively.

2) Two failure modes were observed for the weld-bonded aluminum joint: nugget-through and adherend-tearing. Nugget-through failure was associated with the weld discontinuities, failing primarily by the growth of these discontinuities. Adherend-tearing is induced by the high stress-concentration at the edge of adherend overlap.

3) The fatigue strength of weld-bonded aluminum joints is not significantly affected by the failure modes.

4) For adhesive-bonded aluminum joints, fatigue failure occurred in the form of adherend-tearing at the edge of the adherend overlap.

5) The fatigue strength of weld-bonded aluminum is reduced by the presence of the resistance spot weld. At 3×10^6 cycles, weld-bonded joints show a 11% decrease in the fatigue strength when compared to adhesive-bonded joints.

6) The mechanism of crack growth in the aluminum spot weld is striation. The predominant macroscopic failure mode for aluminum spot welds was identified as nugget pull-out, which is essentially the same as that for the steel spot weld.

Acknowledgment

The authors are grateful to R. Thornton and P. Mabery for the specimen fabrication.

References

1. Abernathy, J. L. 1976. Manufacturing processes for aluminum-steel hoods. SAE paper 760056.

2. Anon. 1976. Aluminum vs. steel for body panels. *Automotive Engineering.*

3. Glaser K. F., and Johnson, G. E. 1974. Construction experience on aluminum experimental bodies. SAE paper 740075.

4. Bartell, B. E. 1976. Automotive sheet metal component conversion from steel to aluminum. SAE paper 760057.

5. Wang, P. C., Frechette, P., Balogh, M., Wong, C., Myers, M., and McEwen, D. 1992. Identification and analysis of epoxy adhesive. Unpublished work, General Motors Corp.

6. Polakowski, N., and Ripling, E. 1966. *Strength and Structure of Engineering Materials,* Prentice-Hall, Inc., Englewood, Cliffs, New Jersey.

7. Abe, H., Kataoka, S., and Satoh, T. 1986. Empirical formula for fatigue strength of single-welded joint specimens under tensile-shear repeated load. SAE Paper 860606.

8. Westgate, S. A. 1978. Resistance welding of aluminum — a literature survey, part II: weldbonding. Welding Institute, report No. 85.

9. Wang, P. C., Chisholm, C., and Mabery, P. 1983. Degradation of fatigue properties of weld-bonded aluminum exposed to moisture and elevated temperature. *Journal of Adhesion,* Vol. 43, pp. 121–137.

10. Welding and Brazing, 1975. *Metals Handbook,* 8th, ASM International, Materials Park, Ohio.

11. Neter, J., and Wasserman, W. 1974. *Applied Linear Statistical Models,* Vol. I, Richard D. Irwin, Inc., Homewood, Ill.

12. Bowker, A. H., and Lieberman, G. J. 1972. *Engineering Statistics,* Prentice-Hall, Englewood Cliffs, N. J.

13. Wang, P. C. 1992. Three-dimensional finite element stress analyses of weld-bonded aluminum joint. Unpublished work, General Motors Corp.

14. McMahon, J. C., and Lawrence, F. V. 1984. Predicting fatigue properties through hardness measurements. Fracture Control Program Report No. 105, University of Illinois at Urbana-Champaign.

15. Wang, P. C., and Ewing, K. M. 1991. A comparison of fatigue strengths: laser beam v. resistance spot welds. *Welding Journal,* pp. 43-47.

16. Ramage, R. M., Kim, C., and Nine, H. D. 1991. Friction coefficients of prelubricated 5754 aluminum alloy sheet against GMR-311, GM-246M nodular iron, and hardened steel. Research Memorandum No. 23-3695/32-2204, General Motors Corp.